

Power Conversion Model and Simulation of Grid Connected Solar and Wind Hybrid System

Saw Ohnmar Oo^{a*}, Lwin Za Kyin^b

^{a,b}*Department of Electrical Power Engineering, Mandalay Technological University Mandalay, Myanmar*

^a*Email: sawohnmar555@gmail.com*

^b*Email: lwinzakysin80@gmail.com*

Abstract

This paper deals with system model, power conversion process, and conversion control of grid connected solar-wind hybrid system. The contribution of the installed PV capacity is 80 kW, and 30 kW of wind turbine which are connected in parallel to a common DC-link bus. As the three levels three stages of voltage source grid inverter is connected to this DC-link bus, the stable bus voltage i.e. 600 VDC is maintained by controlling both of the DC-DC boost converters to the PV side and to the permanent synchronous wind turbine side via a rectifier. The power integration to the utility grid of 11 kV line is performed by the grid inverter through a three phase step-up transformer rated with 400 V/ 11kV, 120 kVA. The power conversion process is taken by considering the variation of solar radiations, PV cell temperatures, and wind speeds. By the help of the power conversion control, the total generated electrical power from the hybrid system can be injected to the utility grid line. In this paper, each of the proposed hybrid system components are developed in MATLAB/Simulink model for observing the feasibility of the available injected power to the grid line under the nature variations of the input power sources. The maximum power point tracking method is approached for getting effectiveness of the available maximum utilization power from the hybrid sources. The control technique of sinusoidal pulse width modulation is applied for generating control pulses of the controllers used in power conversion process. The grid synchronization is performed by the grid inverter control with phase lock loop with grid voltage. This paper mentions and makes discussion briefly about the observations from the simulating results of the proposed overall power conversion model.

Keywords: Grid connected system; Hybrid PV/Wind; Power conversion model; PV System; Wind power system.

* Corresponding author.

1. Introduction

Today's fuel crisis and issues of global warming has increased the demand for renewable energy sources. Conventional energy sources are unable to meet the increasing demand for energy worldwide. Thus, alternative energy sources like sunlight, wind and biomass come into picture. The power generation using the renewable energy sources is advantageous because renewable energy sources are free of cost and maintenance and have longer life. Solar-wind, hydro-wind, wind-diesel, solar thermal-biomass etc. are the well-known hybrid power generation system. The only disadvantage of the solar energy system is that it cannot generate the power in cloudy/rainy days and at night. The performance of the solar system can be improved by integrating the other energy system such as wind power generation system and diesel generator with energy storage. In cloudy days, the solar energy will be less or unavailable, but the favorable wind speed may get on those days, in that case the power requirement will be fulfilled by both of the solar and wind resources. Power generation from hybrid system is much better as it suppresses rapid changes in the output power. In this system there is a wind turbine, the output of the wind turbine goes to permanent magnet synchronous generator. The output of the wind system is in AC, therefore, it needs AC to DC converter to convert the AC output in to DC. Similarly in the PV side the output of the PV array is connected with a DC-DC boost converter to rise the output voltage up to a desire level. And the output of PV and wind are connected with a common DC link voltage. The common DC link voltage will be connected with the DC to AC converter and the output of the inverter is synchronizing with grid. This inverter changes DC power from PV array and the wind turbine into AC power and it maintain the voltage and frequency is equal to the grid voltage and frequency.

2. System components of grid connected solar/wind hybrid system

A hybrid energy system usually consists of two or more renewable energy sources used together to provide increased system efficiency as well as greater balance in utility grid. In this paper, the hybrid energy system is a photovoltaic array coupled with a wind turbine showed in Figure 1. The devices of this hybrid system are PV array, boost converter, MPPT, harmonic reducing filter, IGBT switch, voltage source converter (VSC), wind turbine, a permanent magnet synchronous generator, P.F. correction capacitor and transformer for step up the voltage level. The hybrid system acts as a dominant system and power grid will be act as a standby to compensate the deficit in the hybrid system [1].

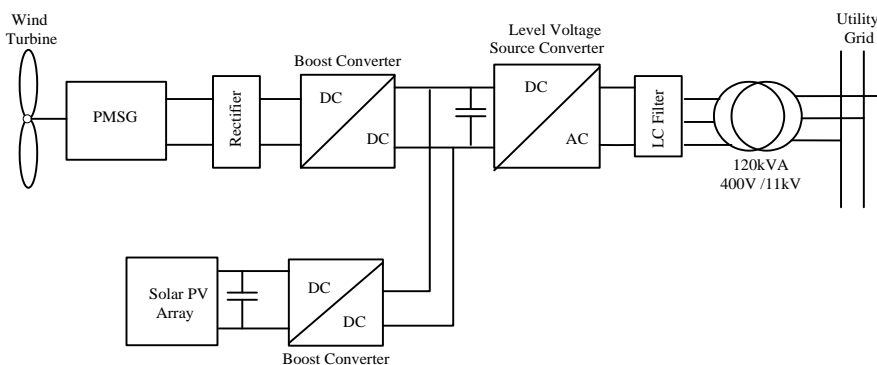


Figure 1: Block diagram of grid connected PV/wind hybrid system

3. Modeling of photovoltaic cell to array

A typical photovoltaic (PV) cell generates an open circuit voltage around 0.5 to 0.7 volts depending on the semiconductor and the built-up technology. Therefore, the cells must be connected in series configuration to form a PV module, to increase the voltage. Further, modules are connected in series and parallel configuration to form an array of desired high voltage and high current. A photovoltaic module is mathematically modelled using single diode equivalent circuit. A mathematical model of single diode PV cell is developed based on current-voltage relationship of a solar cell. An ideal PV cell is represented by a current source and an anti-parallel diode connected to it. A practical PV cell is an addition of equivalent series and a shunt resistance parameter to an ideal PV cell. Fig.1. shows the ideal and practical PV cell of single diode model.

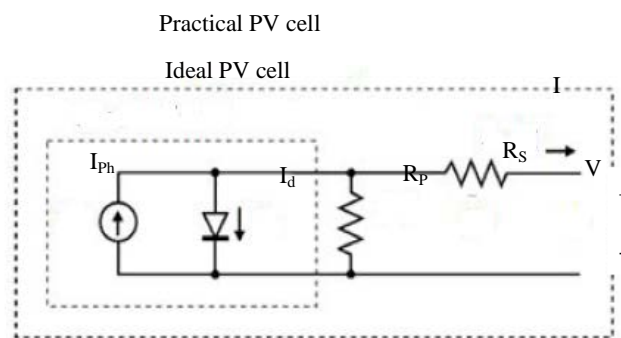


Figure 2: Electrical equivalent circuit model of a PV cell

The effects of solar irradiation and temperature have been considered while designing the PV array. The variation in solar irradiation causes changes in output power and the temperature affects the terminal voltage. The mathematical modeling of the PV array can be given as:

$$I_{ph} = I - I_d - \frac{V}{R_p} \quad (1)$$

$$I_d = I_o \left[\exp\left(\frac{qV_{oc}}{N_s AKT}\right) - 1 \right] \quad (2)$$

$$I_o = I_{rs} \left[\frac{T}{T_r} \right]^3 \cdot \exp\left[\frac{qE_g}{BK} \left\{ \frac{1}{T_r} - \frac{1}{T} \right\} \right] \quad (3)$$

Where, I_{ph} is photon current; I_d is diode saturation current; q is electron charge (1.602×10^{-19}) C; k is Boltzmann's constant (1.381×10^{-23}); T is the PV cell temperature; A and B are PN junction ideality factor; R_s is the series equivalent resistance; R_p is the parallel equivalent resistance, V and I are the photovoltaic output voltage and current respectively [2]. The manufacturer's specifications described in Table 1 are used to evaluate

the behavioural characteristics I-V and P-V under variation of solar irradiation and cell temperature.

$$I = I_{ph}N_p - I_oN_p \left[\exp \left(\frac{V + R_s \left(\frac{N_s}{N_p} \right) I}{V_t a N_s} \right) - 1 \right] - \frac{V + R_s \left(\frac{N_s}{N_p} \right) I}{R_p \left(\frac{N_s}{N_p} \right)} \quad (4)$$

Table 1: Parameters of Kyocera KD-205GX_LP module [3]

Parameters	Rating
Number of PV cells	54
Voltage at P _{max} (V _{mp})	26.6 V
Current at P _{max} (I _{mp})	7.7096 A
Short-circuit current (I _{sc})	8.3596 A
Open-circuit voltage (V _{oc})	33.1999 V
Temperature coefficient of I _{sc}	0.005016
Temperature coefficient of V _{oc}	-0.12
Temperature coefficient of V _{mp} (V/deg.C)	-0.123
Temperature coefficient of I _{mp} (A/deg.C)	-0.001070
Diode ideal factor (A, B)	1.5
Series resistance, R _s	0.15945 Ω
Parallel resistance, R _p	1010.571 Ω

4. Modeling of wind power conversion system

A model of the wind turbine is necessary to evaluate the torque and power production for a given wind speed and the effect of wind speed variations on the produced torque. The torque T and power produced by the wind turbine within the interval [V_{min}, V_{max}], where V_{min} is minimum wind speed and V_{max} is maximum wind speed, are functions of the wind turbine blade radius R, air pressure, wind speed and coefficients Cp and Cq. The power extracted from the wind is given by [4]:

$$P_m = \frac{1}{2} \rho A C_p(\beta, \lambda) V_{Wind}^3 \quad (5)$$

Cp is known as the power coefficient and characterizes the ability of the wind turbine to extract energy from the wind. Cq is the torque coefficient and is related to:

$$C_q = \frac{C_p}{\lambda} \tag{6}$$

$$\lambda = \frac{R \times \omega}{V_{Wind}} \tag{7}$$

Wind turbine output torque (T_m) can be calculated using equation:

$$T_m = \frac{P_m}{\omega} = \frac{1}{2} \rho \pi R^3 C_q V_{Wind}^2 \tag{8}$$

Where, P_m = mechanical output power (watt), β = blade pitch angle, ρ = Air density (kg/m^3), V_{wind} = wind speed (m/s), A = turbine swept area m^2 , λ = tip speed ratio, R = radius of turbine blades (m), T_m = torque of wind turbine, ω = angular frequency of rotational turbine (rad/sec) [5]. The specifications of wind turbine used in the simulation are shown in Table II. Using above equations the Simulink model of wind turbine is implemented as shown in Figure 3.

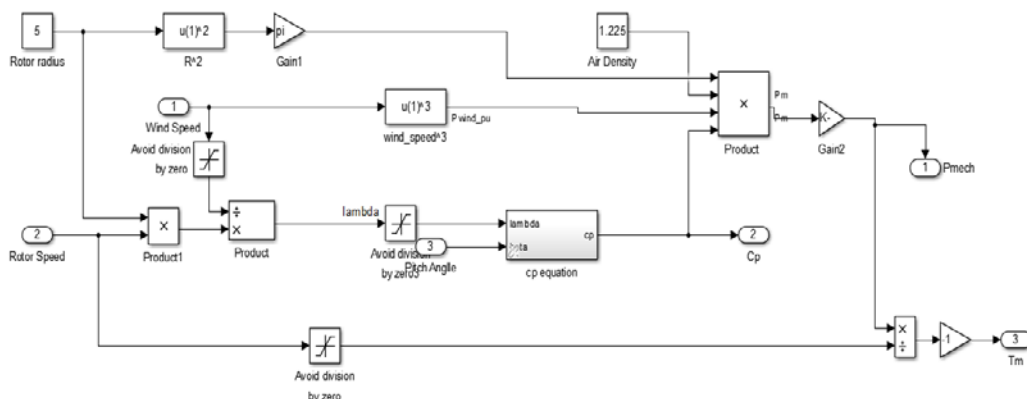


Figure 3: Wind turbine mathematical model

Table 2: Wind turbine specifications [6]

Parameters	Rating
Rated mechanical power, P_m	35 kW
Blade Radius, R	5 m
Number of blades	3
Rated Wind Speed, V_{wind}	12 m/s
Cut in speed, V_i	3 m/s
Cut out speed, V_o	25 m/s
Air Density, ρ	1.225 kg/m^3

The performance coefficient $C_p(\lambda, \beta)$, which depends on tip speed ratio λ and blade pitch angle β , determines how much of the wind kinetic energy can be captured by the wind turbine system. A nonlinear model describes $C_p(\lambda, \beta)$ as:

$$C_p(\lambda, \beta) = C_1 \left(\frac{C_2}{\lambda_i} - C_3 \beta + C_4 \right) e^{-C_5} + C_6 \tag{9}$$

Where $C_1 = 0.5176$, $C_2 = 116$, $C_3 = 0.4$, $C_4 = 5$, $C_5 = 21$, $C_6 = 0.0068$ [7].

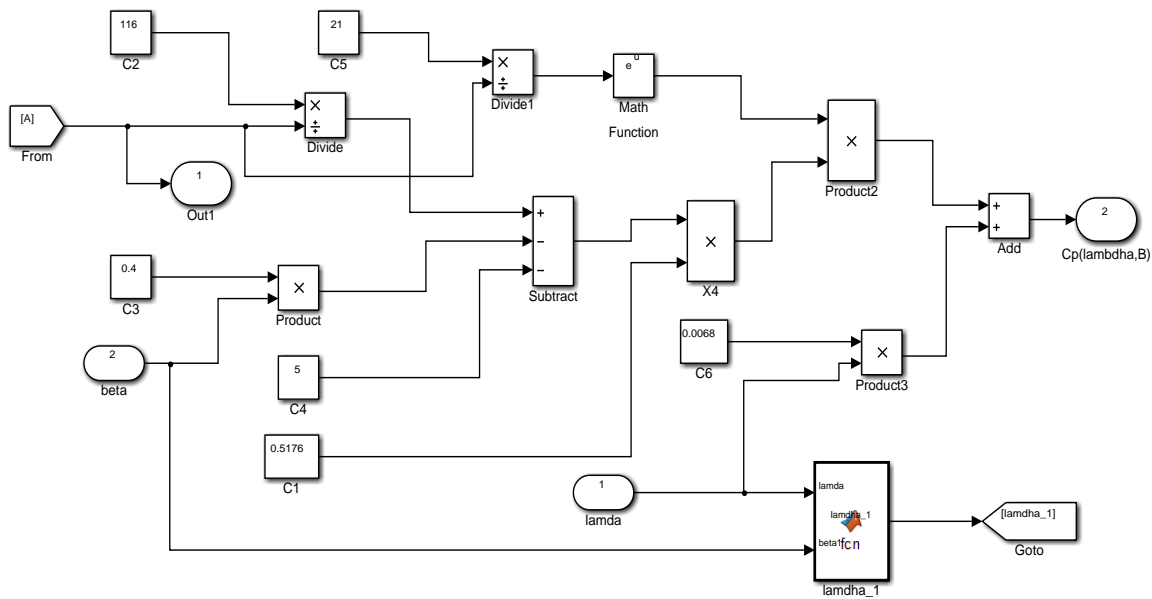


Figure 4: Simulink block of performance coefficient $C_p(\lambda, \beta)$

Figure 4 shows Simulink block of performance coefficient, C_p . The values of C_p were increased when reducing the value of blade pitch angle (degree) β . The maximum value of performance coefficient C_p was obtained when the value of blade pitch angle (degree) β was set to $\beta = 0$. The pitch angle β is controlled only when wind speed exceeds the rated wind speed to maintain the rated output power of the permanent magnet synchronous generator. Otherwise, it is kept constant at $\beta = 0$ for the condition under the rated wind speed.

4.1. Permanent magnet synchronous generator model

Wind turbines generators (WTGs) based on Permanent Magnet Synchronous Generators (PMSG) are becoming popular for variable-speed generation system and the use of the PMSG in large WTGs is growing rapidly. It is connected directly to the turbine without gearbox and so it can operate at low speeds [4].

But it can generate desire output power at rated wind speed. The parameters of PMSG used in the simulation are shown in Table 3.

Table 3: Specifications of PMSG [8]

Parameters	Rating
Rated Power, P_e	30 kW
Rated line Voltage, V_L	400 V
Rated frequency, f	50 Hz
Stator phase resistance, R_s	0.056 Ohm
Armature inductance, L_a	0.0016 H
Number of poles, P_n	32

The mathematical model of a PMSG is usually defined in the rotating reference frame d-q as follows:

$$V_{gq} = (R_g + p.L_q).i_q + \omega_e L_d i_d + \omega_e \psi_f \tag{10}$$

$$V_{gd} = (R_g + p.L_d).i_d - \omega_e L_q i_q \tag{11}$$

Where V_{gd} and V_{gq} are the direct stator and quadrature stator voltage, respectively. i_d and i_q are the direct stator and quadrature stator current, respectively. R_g is the stator resistance, L_q and L_d are the inductances of the generator on the q and d axis, ψ_f is the permanent magnetic flux and ω_e is the electrical rotating speed of the generator, defined by:

$$\omega_e = P_n \omega_m \tag{12}$$

Where P_n is the number of pole pairs of the generator and ω_m is the mechanical angular speed. The electromagnetic torque can be described as:

$$T_e = \frac{3}{2} P_n [\psi_f i_q - (L_d - L_q) i_d i_q] \tag{13}$$

If $i_d = 0$, the electromagnetic torque is expressed as:

$$T_e = \frac{3}{2} P_n \psi_f i_q \tag{14}$$

The power of the generator is calculated as:

$$P_e = T_e \omega_e \tag{15}$$

5. Modeling and control of dc-dc boost converter

The boost converter is a medium of power transmission to perform energy absorption and injection from solar

panel to the DC-link. The circuit components of the boost converter consist of inductor, IGBT, diode, output capacitor and load resistor as shown in Figure 5. The duty cycle for boost process will depend on the desire output voltage, the minimum and maximum input voltage range of the boost converter.

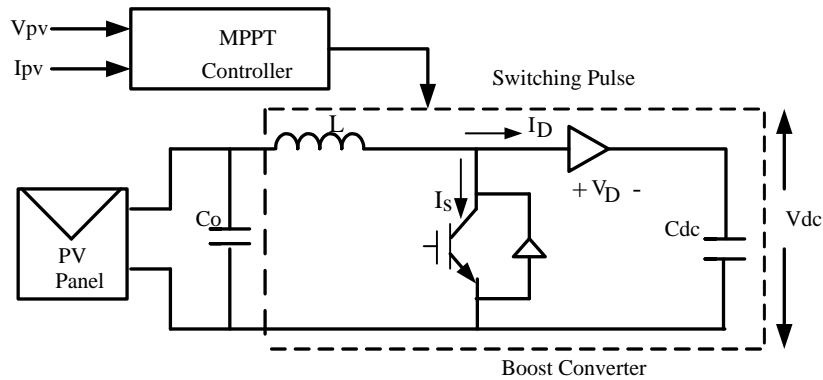


Figure 5: Circuit diagram of DC-DC boost converter [9]

In order to determine the value of minimum inductor L_{min} and minimum capacitor C_{min} of the boost converter, the switching frequency of the boost controller should be properly taken to achieve the output voltage with less harmonics. The minimum and maximum duty cycles, the L_{min} and C_{min} value expressed for continuous conduction mode operation can be obtained as follows:

$$D_{min} = 1 - \frac{V_{imax}}{V_o} \quad (16)$$

$$D_{max} = 1 - \frac{V_{imin}}{V_o} \quad (17)$$

$$L_{min} = \frac{2}{27} \times \frac{R_{Lmax}}{f_s} \quad (18)$$

$$C_{min} = \frac{D_{max} V_o}{f_s R_{min} V_r} \quad (19)$$

Where, V_r is the ripple factor of output voltage. In this case, the ripple factor is considered as 5% [10]. Filter circuits use either capacitor or inductor or both to limit the ripple. Here, filter capacitor (100 μ F) is used to eliminate the ripples. The chosen ratings according to it's minimum value of inductor and capacitor for PV side boost converter are 1 mH and 3500 μ F. These parameters are applied to the simulation model shown in Figure 6 which has controlled to yield constant DC output of 600V by varying the duty cycle ranged from 0.71 to 0.5 in response to variations of DC input voltage ranged from minimum 196V to maximum 250V.

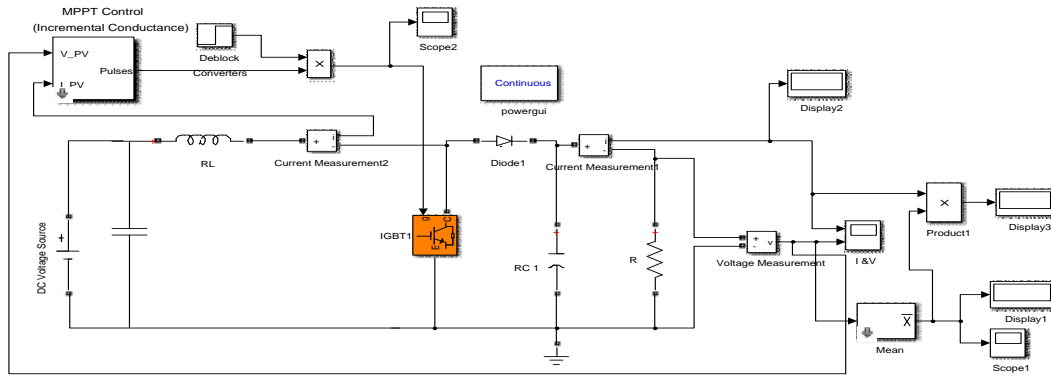


Figure 6: Simulink model of DC-DC boost converter

There are some methods used for maximum power point tracking: Perturb and Observe (P&O) method, Incremental Conductance (INC) method, Parasitic Capacitance method, Constant Voltage method, Constant Current method. Of all these methods, Incremental Conductance method tracks rapidly changing irradiation conditions more accurately than P&O method, whereas the basic of INC method comes from P&O algorithm [11]. The MPPT algorithm used in this work is the incremental conductance method where the change in current, change in voltage, instantaneous voltage and instantaneous current values are taken into account to do the necessary duty cycle variations. The voltage and the current of the photovoltaic array are the input of MPPT algorithm and the duty cycle is the output of it. The MPPT simulation block is shown in Figure 7. The duty cycle is compared to a triangle wave signal to generate the PWM.

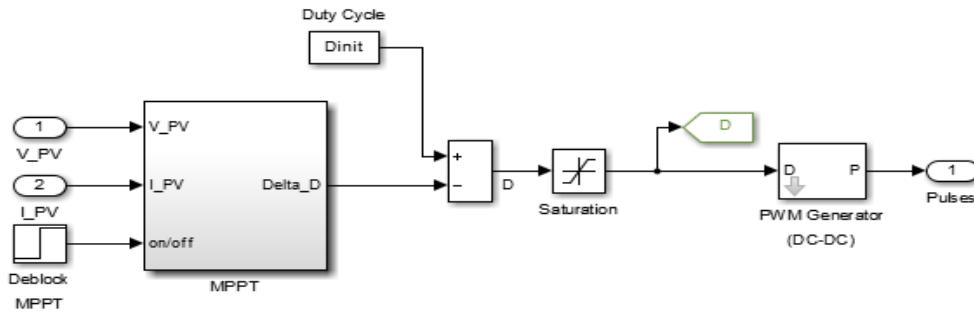


Figure 7: MPPT simulink model

The PWM control signal is applied to the gate terminal of IGBT switching device. The MPPT regulates the PWM control signal of the boost converter until the condition: $(dI/dV) + (I/V) = 0$ is satisfied. According to INC method, there is a single peak value on the P-V characteristic curve and the maximum power point exists where:

$$\frac{dP}{dV} = 0 \tag{20}$$

$$\frac{dP}{dV} = \frac{d}{dV}(V \times I) = 0 \tag{21}$$

$$\frac{dP}{dV} = I + \frac{dI}{dV} = 0 \quad (22)$$

$$\frac{dI}{dV} = -\frac{I}{V} \quad (23)$$

According to the relationship between $\frac{dI}{dV}$ and $\frac{I}{V}$ operating voltage can be adjusted and maximum power point can be achieved. If, $\frac{dI}{dV} < -\frac{I}{V}$ then the operating point is at the right hand side of the MPP, and the output voltage of the PV should be reduced in this case. Similarly if, $\frac{dI}{dV} > -\frac{I}{V}$ then, the operating point is at the left hand side of the MPP, and the output voltage of the PV should be increased for this condition [12].

On the other hand, the wind generator side converter contains three phase diode rectifier and DC- DC boost converter. The generated AC power is first rectified using uncontrolled rectifier, and then DC/DC boost converter is controlled by PWM techniques to link the common DC bus voltage. The relation between the input and output voltage and currents of the boost converter is expressed by the following equation [13]:

$$V_{dc2} = \frac{I}{1-D} V_{dc1} \quad (24)$$

Where V_{dc1} and V_{dc2} are the input and output voltage of the boost converter which design parameters are based on getting the constant DC link voltage. The rectified DC voltage will ranged from minimum 150 V to maximum 566 V. By taking the switching frequency as 1 kHz, the boost controller will operate with duty cycle varied from 0.15 to 0.78 to give the desire DC link voltage i.e.600V. The design parameters for the wind side boost converter are considering with the previous equations, and taking values as 10 mH for inductor, 3500 μ F for capacitor. For eliminating the output ripples, 1300 μ F of filter capacitor is applied in the simulink model.

6. Modeling the three level inverter and control interface with grid line

The grid side inverter is connected to the common DC link of the proposed PV/Wind hybrid system. A three-level inverter consists of two capacitor voltages in series, and uses the center tap as the neutral. One leg consists of two pair of IGBTs/diodes and two diodes. The configuration circuit diagram for three phase three level diode clamped inverter is shown in Figure 8. The conversion unit which performs the interface functions between the DC bus and three phase AC grid followed by the L filter converts the energy to the utility grid. The value of DC link voltage and the grid line voltage are related as in the following equation:

$$0.612m_a V_{dc} \geq \sqrt{(V_{ac})^2 + 3(\omega_f I_{ac})^2} \quad (25)$$

The control option for grid interface is aimed to adjust the active power and reactive power delivered to the grid. The Simulink model of the grid side converter control system is shown in Figure 9. The control parameters are

V_{dc} , grid voltage V_{abc} , grid current I_{abc} and reference dc-link voltage V_{dc_ref} . The complete control system is divided into two parts: voltage regulator and current regulator. The output of the control system provides the reference signal, used as the input for the PWM signal generator which gives the firing pulse for controlling the grid side converter. For each sample time V_{dc} is measured and compared with V_{dc_ref} until the voltage across the grid is regulated to the desired voltage [14]. Equations (26) to (28) are used in modeling PI controller for voltage regulation. As in Figure 10, the voltage controller which k_p and k_i values of the PI controller are 7 and 800 respectively regulates the inverter output voltage with grid voltage by controlling the DC link voltage to get the stable voltage.

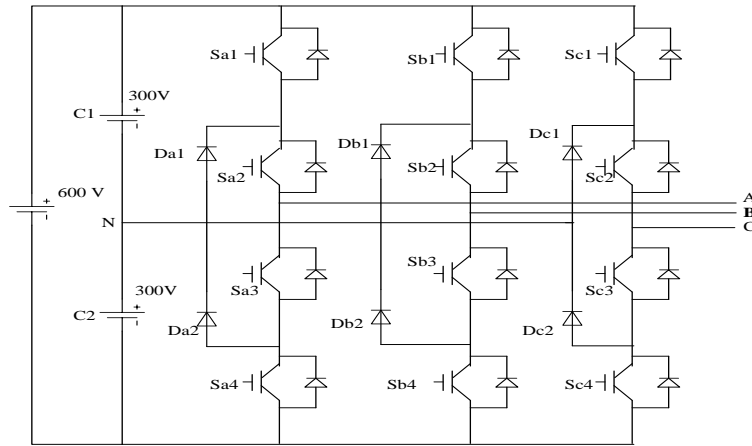


Figure 8: Three phase three level voltage source inverter

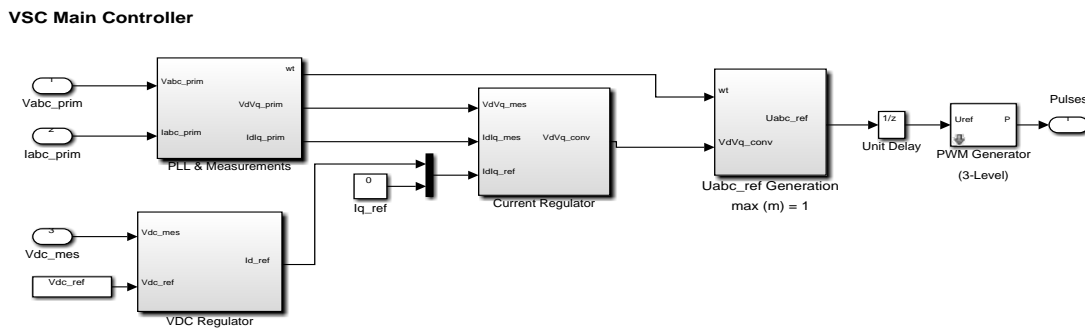


Figure 9: Simulation model for grid side voltage source converter control system

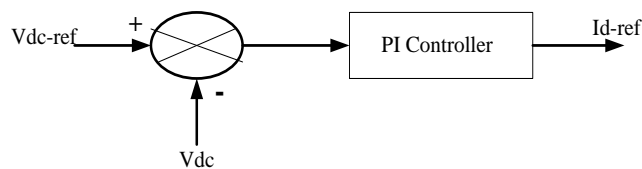


Figure 10: Voltage controller

$$V_{dc-error} = V_{dc-ref} - V_{dc} \tag{26}$$

$$I_{d-ref} = K_{p-Vdc} (V_{dc-error}) + K_{i-Vdc} \int (V_{dc-error}) dt \tag{27}$$

$$I_{q-ref} = 0 \tag{28}$$

Where V_{dc} , V_{dc-ref} , $V_{dc-error}$ are dc-link voltage, reference dc-link voltage and dc-link voltage error respectively. I_{d-ref} , I_{q-ref} are reference d and q current components respectively. K_{p-Vdc} , K_{i-Vdc} are proportional and integral constant value of the PI controller. Equation (29) to (33) are used for developing the current regulator as shown in Figure 11. The K_{p-CR} , K_{i-CR} of the PI controller of current regulator are for 0.3 and 20 respectively to provide V_d' and V_q' . I_d and I_q are the d and q current components respectively, obtained using park transformation (abc to dq0) for the three phase grid current $I_{abc-grid}$. The control voltage $V_{control-grid}$ used for PWM generation is obtained by applying transformation to provide V_d' and V_q' [15].

$$I_{d-error} = I_{d-ref} - I_d \tag{29}$$

$$V_d' = V_d [K_{p-CR} (I_{d-error}) + K_{i-CR} \int (I_{d-error}) dt] + LI_q \tag{30}$$

$$I_{q-error} = I_{q-ref} - I_q \tag{31}$$

$$V_q' = -[K_{p-CR} (I_{q-error}) + K_{i-CR} \int (I_{q-error}) dt] + LI_d \tag{32}$$

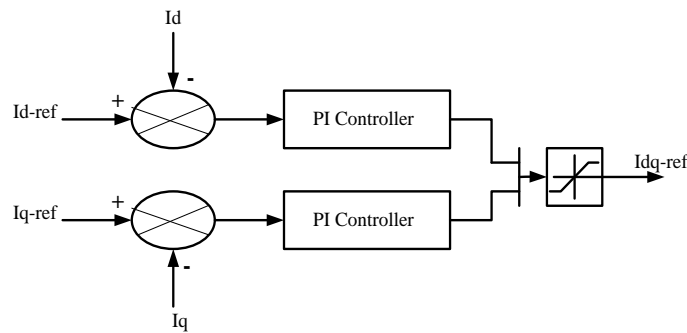


Figure 11: Current controller

Synchronization of inverter with the grid line is done by Phase Locked Loop (PLL) as shown in Figure 12. Using PLL control, the phase angle difference (δ) between inverter voltage (V_{inv}) and the grid voltage (V_{grid}) will reduce to 0 [16]. The accurate control of synchronism can be done noise proof with respect to the grid by sensing the grid voltage in a phase locked loop. The PLL output is the actual angle position of the grid voltage. By controlling δ , the real and reactive power flow to grid line can be obtained as follows:

$$P = \frac{V_{inv} V_{grid}}{X_L} \sin \delta \tag{33}$$

$$Q = \frac{V_{inv}}{X_L} (V_{inv} - V_g \cos \delta) \tag{34}$$

Where, X_L is the connected impedance involved with the transformer leakage impedance and coil impedance. The main problems of operating hybrid system are involved with system stability and power quality. By taking improvement for inverter's gate pulse control and synchronization process, these problems can be eliminated significantly for the grid-connected option. The system synchronizing between the hybrid system and grid line satisfies with matching frequency, voltage phase sequence, and magnitude [17].

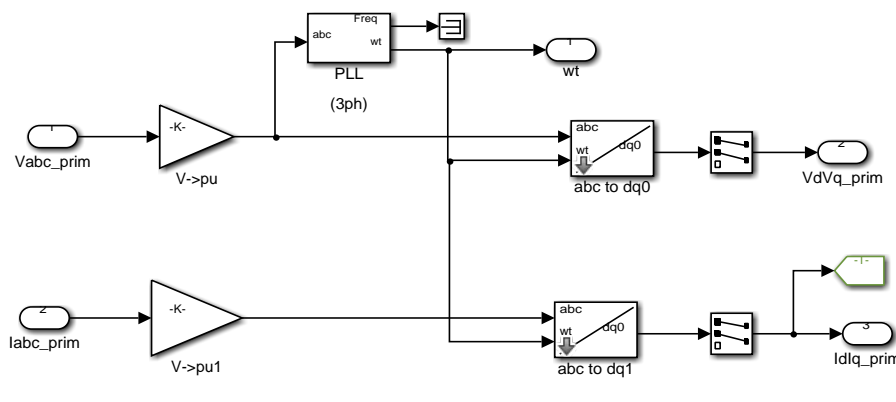


Figure 12: Phase Locked Loop synchronization unit

7. Overall simulation model and results

The grid line voltage levels used for power distribution and transmission network in Myanmar are 500 kV, 230 kV, 132 kV, 66 kV, 33 kV and 11 kV lines. This research work is implied for distribution level, and 11 kV is chosen for testing the system performance with Matlab/Simulink model. The overall simulation model of the grid connected solar and wind hybrid system is shown in Figure 13. In this research work, the total installed capacity of the proposed hybrid system is studied for 110 kW which contributes 30 kW of wind turbine generator and 80 kW of PV generator. Both the systems are considered to operate in parallel during day time, and but for night time, only the wind generator has to serve for the power conversion purpose.

The proposed hybrid simulation model is tested for different conditions of change in wind speed, change in solar irradiation, and change in cell temperature. The array composed of 39 parallel strings with each containing 10 modules in series to obtain terminal voltage of 260V i.e suitable for grid connection purposes. The PV array formed by Kyocea KD205GX-LP modules provides maximum power of 79.27 kW and 270 V under standard test conditions. Figure 14 shows the I-V and P-V characteristic curves at different levels of solar irradiance when cell temperature is constant at 25°C. With increasing cell temperature with constant solar irradiation, the voltage at maximum power point decreases from 270 V to 200 V with increasing the temperature from 25°C to

75°C as shown in Figure 15. cell temperature constant at 25°C

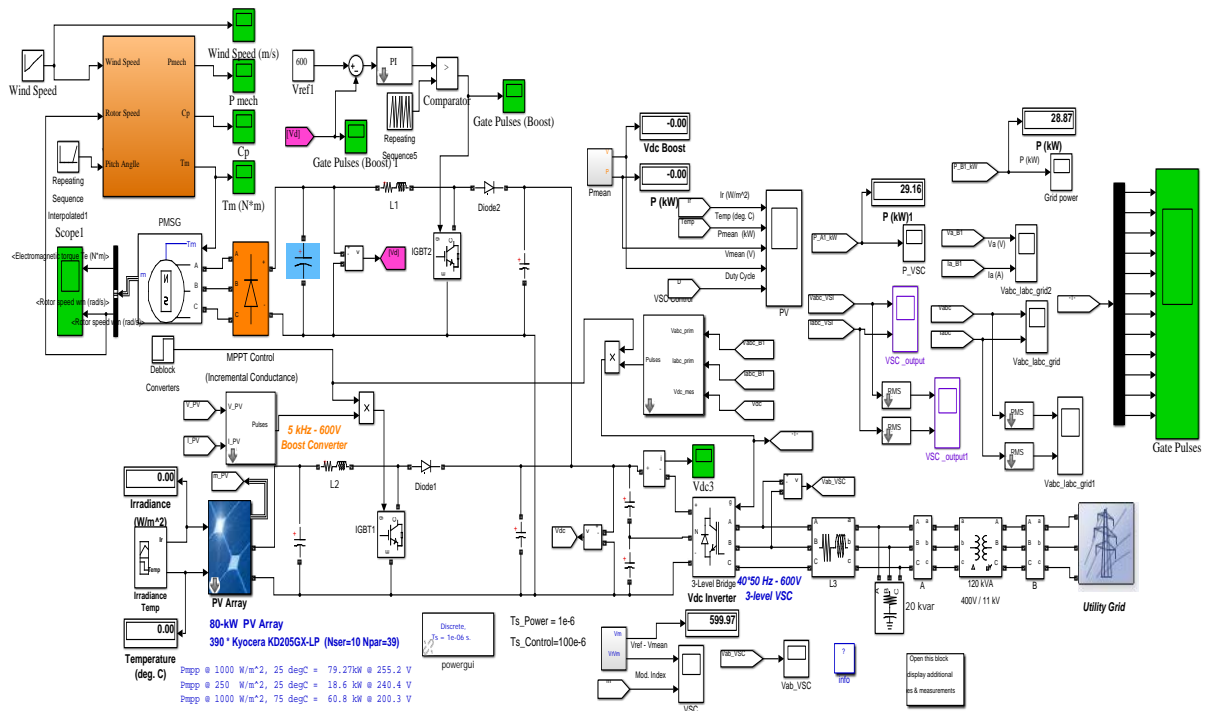


Figure 13: Overall simulation diagram of grid connected wind /PV hybrid system

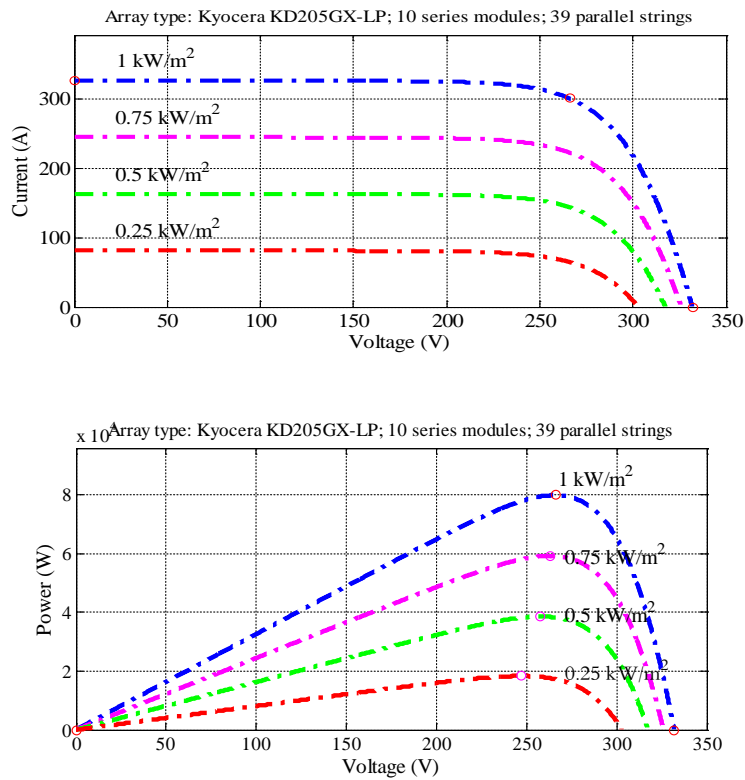


Figure 14: Characteristic curves of PV array for different solar irradiance levels with

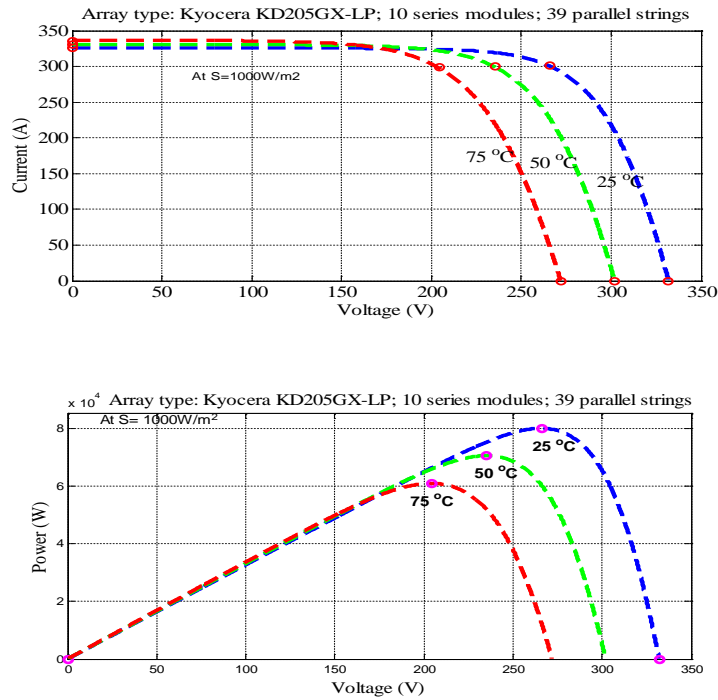


Figure 15: Characteristic curves of PV array for different cell temperatures with

solar irradiance level constant at 1000 W/m^2

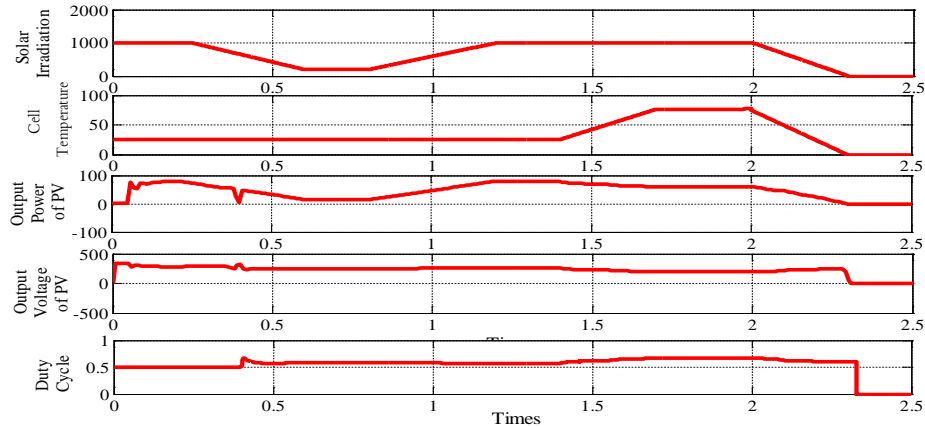


Figure 16: Simulation results with mean value for PV generator input and output

By taking simulation results as seen in Figure 16, the system performance under temperature and solar radiation changing condition can be investigated for the available power conversion process to connect to grid line. The wind speed of the wind turbine and mechanical power are presented in Figure 17. This variation in wind speed affects the electrical power produced by the PMSG coupled to the wind turbine as observed in Figure 18. The DC link voltage is maintained constant by the boost controllers although the wind generator output voltage is changed with respect to wind speed changes, and the PV generated output is changed due to the variation of solar radiance levels and cell temperatures. The DC link capacitor takes about 0.5 seconds to get the steady state voltage of 600 VDC, and the modulation index are shown in Figure 19. The voltage source converter control

system uses an external control loop which regulates DC link voltage to +/- 300 VDC, and the active and reactive current components of the grid current is to be regulated by the internal control loop.

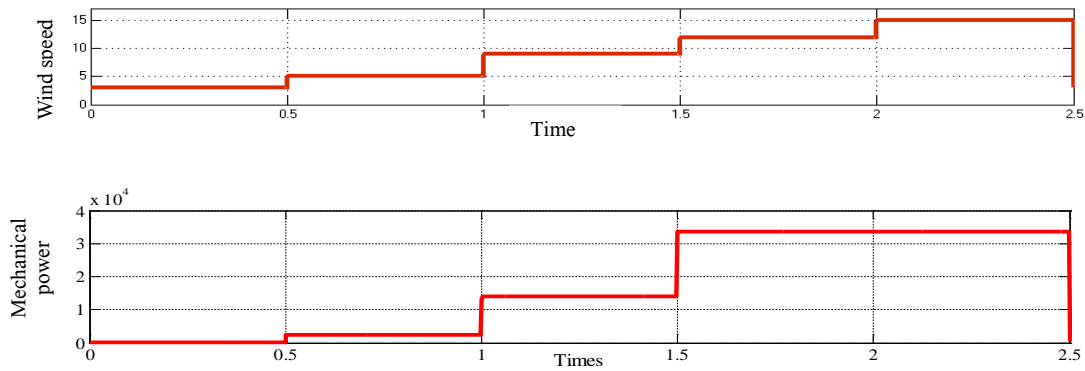


Figure 17: Simulation results for mechanical power output according to different wind speeds

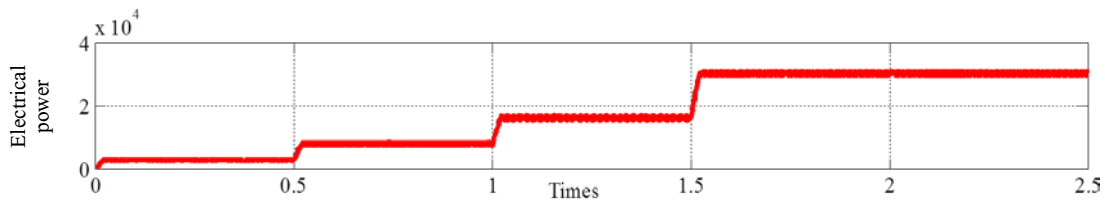


Figure 18: Simulation result of electrical output power of 30 kW PMSG wind generator

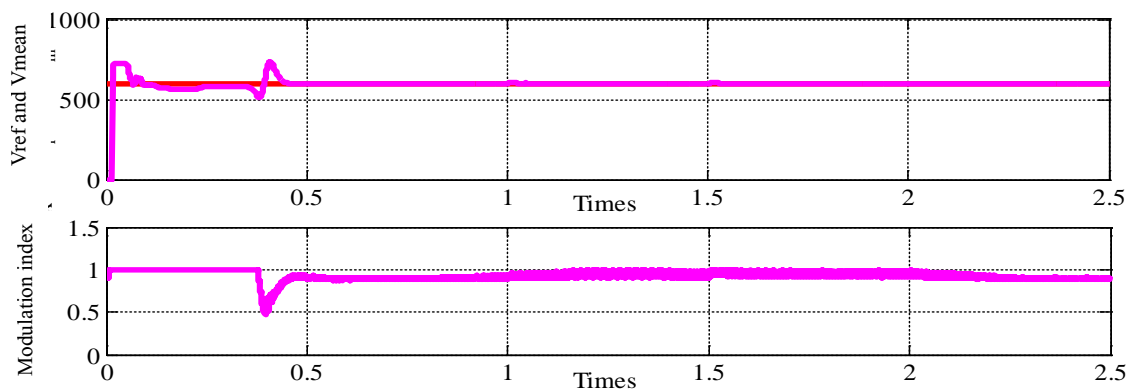


Figure 19: DC link capacitor voltage and modulation index

The PWM control techniques is applied to control the switching pulses of voltage source inverter with 2 kHz frequency. To suppress the harmonic contents of the inverter output current, 15 kvar capacitor bank is implemented at the output of the inverter. After filtering harmonic contents, the inverter output line current and voltage observed at the input terminal of the step-up 400 V/11 kV transformer are simulated in Figure 20. The harmonic contents of the transformer output current is 1.77% which is found by FFT analysis. After injecting the solar/wind hybrid generated power to the utility grid line of 11 kV, the simulation results for synchronization voltage and current are observed as shown in Figure 21 and Figure 22.

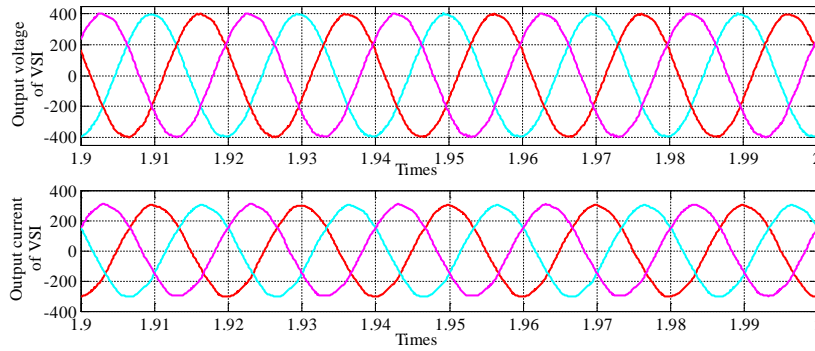


Figure 20: Line current and voltage at input terminal of 400V/11kV transformer

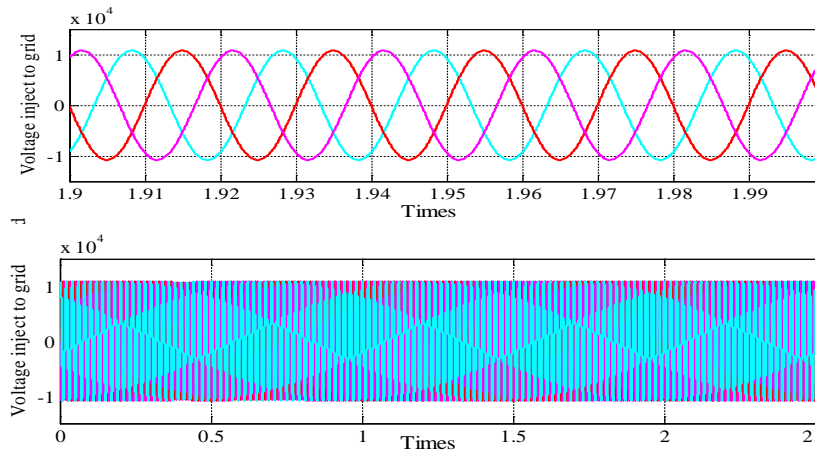


Figure 21: Simulation results of synchronization voltage to 11kV grid line

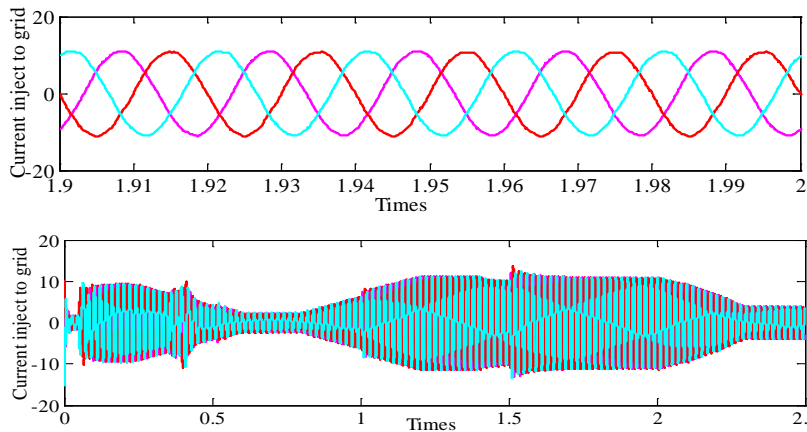


Figure 22: Simulation results of synchronization current to 11kV grid line

The overall injected power to the grid is plotted in Figure 23 which gives the maximum overall system efficiency of 74%. Maximum output power of hybrid system to grid is obtained 81 kW which shows the converter loss is 29 kW. The grid voltage is maintained at peak voltage 11 kV, 50 Hz. During that period, the current flowing on the grid line gets its maximum value. But for the duration of significantly decreasing cell

temperature and solar irradiance up to zero, the system can inject power to the grid line from only wind generation source which produces 28 kW at rated wind speed.

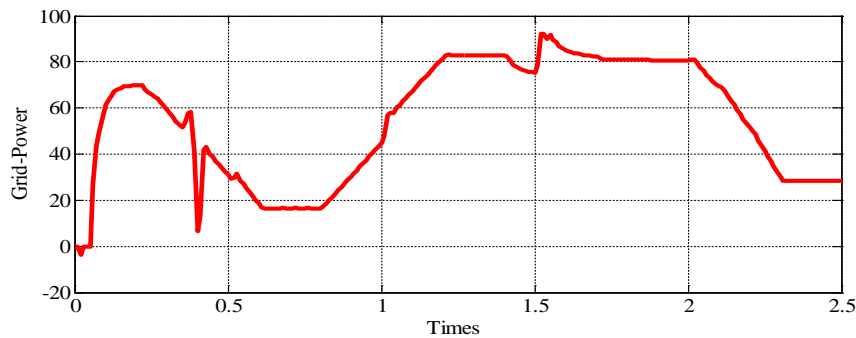


Figure 23: Injected power to the grid

8. Discussion and conclusion

A complete description of the hybrid system has been presented along with its detailed simulation results which ascertain its feasibility. This research work is performed by taking consideration with the existing utility grid line which allows integration of injected power from the PV-wind hybrid system. The grid connected option for the proposed solar/wind hybrid system is implemented by taking variations of sunlight irradiance, PV cell temperature and wind speeds as input parameters. As for having less complexity control topology compared to the AC linked hybrid system, a common DC linked bus is chosen to maintain stable at 600V by controlling the boost converters of PV side and wind side respectively. The synchronization process for power injection to the utility grid line of 11kV is performed successfully with grid inverter through the 120 kVA 400 V/11 kV three-phase coupling transformer. In this research work, the maximum available total power injected to grid line i.e. 81kW has observed by simulating the generated power under standard solar irradiation with rated wind speed. The total install capacity i.e 110 kW of the proposed hybrid system gives the overall power conversion efficiency of 73%. Considering to reduce harmonic effects on the converter efficiency, the design parameters for the boost converters and inverters were calculated for the power conversion model in Matlab/Simulink.

Considering on the advantages of power electronic control devices, the design data and control strategies are applied for conversion control process. The grid inverter performs grid synchronization process with phase lock-loop control method which is an important function for leading this research work successful. The overall system model was simulated, and observed for the system performance of the proposed hybrid system. From these simulation results, the impacts of voltage drop in PV generator due to cell temperature rise was found reasonably to decrease the injected power to the grid. Although the nature variations of the solar radiation level and wind speed are uncontrollable parameters, the generated power fluctuation can be converted by taking control properly for grid connected option.

As being less dependent on the environmental condition as compared to the power generated of individual PV or wind generation system, the proposed PV/Wind hybrid system can give the more reliable power supply source

for grid-connected option throughout the year. However, there would be some constraints for supply sources condition related to the hybrid system operation. Aspecially for night time and cloudy or no sun day, if the wind turbine also is not able to produce sufficient power for feeding the grid conversion process, the system has to be shutdown frequently during that periods. Therefore, it is recommended that the grid connected PV/wind hybrid system should have battery backup system which can also improve to suppress the power fluctuation. Furthermore, the grid inverter should be controlled with space vector pulse width modulation control method to improve output voltage waveforms, smaller filter size and to minimize the total harmonic distortions.

Acknowledgments

The author is deeply gratitude to Dr. Myint Thein, Rector, Mandalay Technological University, for his guidance and advice. The author would like to thank to Dr. Yan Aung Oo, Professor and Head, Department of Electrical Power Engineering, Mandalay Technological University, for his kind permission, providing encouragement and giving helpful advices and comments. The author is grateful to her supervisor, Dr. Lwin Za Kyin, Associate Professor, Department of Electrical Power Engineering, Mandalay Technological University, for her invaluable supervision, helpful suggestion and necessary assistance throughout the preparation of this research work.

References

- [1] Md. SifatFerdous Chowdhury and Mohammad Abdul Mannan “Simulating Solar and Wind Based Hybrid Systems Synchronized and Segmented for Grid Connectivity” International Journal Of Multidisciplinary Sciences And Engineering, VOL. 5, NO. 8, AUGUST 2014.
- [2] A issa Chouder et al. 2011. Modeling and simulation of a grid connected PV systems based on the evaluation of main PV module parameters, Sciverse Science Direct.
- [3] website: <http://www.ghrepower.co.uk/> , last date accessed 1\11\2016
- [4] Shun Yang, Lida Zhang, (2013)"Modeling and Control of the PMSG Wind Generation System with a Novel Controller" Third International Conference on Intelligent System Design and Engineering Applications (ISDEA), pp.946-949, 16-18 Jan. 2013.
- [5] Shao Zhang, King-Jet Tseng, D. Mahinda Vilathgamuwa, Trong Duy Nguyen and Xiao-Yu Wang, Design of a Robust Grid Interface System for PMSG-Based Wind Turbine Generators, IEEE Transactions On Industrial Electronics, Vol. 58, No 1, pp.316-328 , January 2011.
- [6] website: [http://www.m.zonhan.com/Shanghai Ghrepower Green Energy Co.Ltd](http://www.m.zonhan.com/Shanghai_Ghrepower_Green_Energy_Co.Ltd) , last date accessed 1\11\2016
- [7] Dr. A.K.Pandey and Aditi “Performance Analysis of grid connected PV Wind Hybrid Power System” International Journal of Applied Engineering Research ISSN 0973-4562 Volume 11 @ Research India

Publications.

- [8] Zakariya Dalala, "Design and Analysis of a Small-Scale Wind Energy Conversion System" November 13th, 2013 Blacksburg, VA .
- [9] S. Kolsi, H. Samet and M. Ben Amar, "Design Analysis of DC-DC Converters Connected to a Photovoltaic Generator and Controlled by MPPT for Optimal Energy Transfer throughout a Clear Day", *Journal of Power and Energy Engineering*, 2014, 2, 27-34 Published Online January 2014.
- [10] N. Mohan, T. Undeland, and W. Robbins 'Power Electronics Converters, Application and Design', New York: John Wiley & Sons, 2003.
- [11] M. K. Gupta, Rohit Jain, Anjali Goswami, "Design & Simulation Of Photovoltaic System Using Advance Mpppt", *International Journal of Advanced Technology & Engineering Research (IJATER)* July 2012.
- [12] K. T. Tan, P. L. So, Y. C. Chu, and K. H. Kwan. Modeling, Control and Simulation of a Photovoltaic Power System for Grid-connected and Stand-alone Applications. *Proceedings of IPEC, IPEC'10*, pp 608-613, 2010.
- [13] P.A. Stott, M.A. Mueller, V.D. Colli, F. Marignetti, R. Di Stefano, (2007) "DC Link Voltage Stabilisation in Hybrid Renewabl Diesel Systems, International Conference on Clean Electrical Power, 2007 ~ICCEP '07~, pp.20-25.
- [14] F Valenciaga and P Puleston, "Supervisor control for a stand-alone hybrid generation system using wind and photovoltaic energy," *IEEE Transactions on Energy Conversion*, vol. 20, no. 2, pp. 398-405, 2005
- [15] Vigneshwaran Rajasekaran, "Modeling, Simulation and Development of Supervision Control System for Hybrid Wind Diesel System" July 19th, 2013.
- [[16] Adzic, E., M. Adzic and V. Katic, 2011. "Tuning of Grid Synchronization Unit for Distributed Power Generation Systems", in *Proc. ETRAN 2011*.
- [17] Hanif, M.: Investigation to Improve the Control and Operation of a Three-phase Photovoltaic Grid-tie Inverter. Doctoral Thesis. Dublin Institute of Technology, 2011.